State-Selective Predissociation Spectroscopy of HCl^+ and DCl^+ Ions†

Michael Michel,‡ Mikhail V. Korolkov,§ and Karl-Michael Weitzel*,‖

Institut für Chemie, Freie Universität Berlin, Takustrasse 3, 14195 Berlin, Germany, Academy of Science, Stephanov Institute of Physics, Minsk, Belarus, and Fachbereich Chemie, Institut für Physikalische Chemie, Philipps Universität Marburg, Hans Meerwein Strasse, 35032 Marburg, Germany

Received: May 7, 2004; In Final Form: June 17, 2004

The state-selective predissociation spectroscopy of HCl^+ and DCl^+ ions has been investigated in a two color double-resonance experiment. Ions are formed in the vibronic ground state $\tilde{X}\ ^2\Pi_{3/2}$ by the first laser via resonance enhanced multiphoton ionization. Predissociation of these ions is induced by excitation to the excited $A\ ^2\Sigma^+$ state. Analysis of the predissociation spectra is shown to provide access to (i) the spectroscopic parameters of the electronic states involved, (ii) the lifetime of the predissociating states, and (iii) the rotational state distribution of the ions.

1. Introduction

Experiments with state-selected molecules contribute significantly to the detailed understanding of chemical reactions.[1−3] For neutral molecules, state selection is—in principle—easily defined by a state-selective optical excitation, where the question of separation from unexcited molecules may still pose a technical problem. For molecular ions the separation from unexcited, neutral molecules is not a fundamental problem, but the preparation of state-selected molecular ions is less straightforward. In particular the preparation of such ions by optical means involves the ejection of a photoelectron. Here, the transfer of angular momentum to the electron is possible. This in general leads to the situation that ions are formed in at least two different rotational quantum states. In the following we still term such ions as state selected, provided that the center of the rotational state distribution can be shifted in a controllable fashion. Besides from the threshold and pulsed field ionization techniques, there is one remarkably simple technique for the formation of molecular ions with very narrow rotational state distribution (i.e., resonance enhanced multiphoton ionization; REMPI).[4] REMPI spectra are known for a large number of molecules. But only for some examples quantitative information on the rotational state distribution is available.[5] This lack of information is probably due to the techniques routinely employed today. Information on the rotational state distribution can be derived from titrating back the electrons formed in a REMPI process by photoelectron spectroscopy (PES).[6,7] This provides rotational resolution for large rotational quantum numbers in small molecules. For low rotational quantum number, the resolution of PES is in general not sufficient. A different approach is based on the projection of the distribution of interest onto a final state with significantly different spectroscopic parameters. If a predissociative final state is chosen, this opens the possibility to record an action spectrum by measuring the fragment ion yield as a function of the excitation energy. In recent work, we have quantitatively investigated the rotational state distribution of HBr^+ ions formed via two different REMPI transitions by state-selective predissociation spectroscopy.[8] We found that, for each pump line in the rotationally resolved REMPI spectrum, ions are formed in a well-defined narrow rotational state distribution whose center can be shifted by choosing the appropriate pump line.

A homologous prototypical system is the HCl molecule, for which also a large body of spectroscopic information is available, including Rydberg state spectroscopy[9−11] and classical photoelectron spectroscopy.[12−14] By means of laser photoelectron spectroscopy, de Lange and co-workers showed that molecular ions can be formed in rather high rotational states via a REMPI process.[7,15] The distribution of states appeared to be narrow; however, quantitative state distributions were not derived. In previous work of our group, we have investigated the formation of HCl^+ ions via the $f\ ^3\Delta_2 \leftarrow \tilde{X}\ ^1\Sigma^+$ REMPI transition.[16] The rotational state distribution was derived from projecting the ion ground state onto a dissociating state. In that work the $A\ ^2\Sigma^+$ ($v' = 6$) state was employed, which turned out to be correlated with two photon dissociation spectroscopy. The relevant transition moments had not been taken into account.

In the current work, we present an extended investigation of the state distribution of HCl^+ ions formed via the $f\ ^3\Delta_2 \leftarrow \tilde{X}\ ^1\Sigma^+$ (2+1) REMPI transition. Here, we again apply predissociation spectroscopy; however, since we employ the $A\ ^2\Sigma^+$ ($v' = 7$) state, we are strictly looking at one photon predissociation. Consequently, we are able to take into account the relevant transition moments. Compared to previous work, we have now investigated a larger range of pump lines in the REMPI spectrum. The data for HCl^+ are compared to that for DCl^+.

2. Experimental Technique

HCl molecules from an effusive beam are ionized in the ion source of a linear time-of-flight mass spectrometer (TOF-MS)[17] via the $f\ ^3\Delta_2 \leftarrow \tilde{X}\ ^1\Sigma^+$ (2+1) REMPI transition at wavelength λ_1. After a delay of 15 ns, these ions are further excited by a second laser into the $A\ ^2\Sigma^+$ state, which predissociates by spin−orbit coupling to three repulsive electronic states ($^4\Sigma^-$, $^2\Sigma^-$, and $^4\Pi$).[18] The ions are mass analyzed in the TOF-MS. Predissociation spectra are recorded by detecting fragment ions Cl^+ as a function of the wavelength (λ_2). Note that this experiment is

† Part of the special issue "Tomas Baer Festschrift".

* Corresponding author e-mail: weitzel@chemie.uni-marburg.de.
‡ Freie Universität Berlin.
§ Stephanov Institute of Physics.
‖ Philipps Universität Marburg.

10.1021/jp048042n CCC: $27.50
Published on Web 07/29/2004

not sensitive to the substates of the Cl^+ (^3P_j, $j = 0, 1, 2$). However, close to the threshold of predissociation spin−orbit coupling to the $^4\Sigma^-$ state should dominate, which would lead to the formation of Cl^+ ($^3P_2$). The $^2\Sigma^-$ repulsive state correlates with Cl^+ ($^3P_1$), the $^4\Pi$ repulsive state correlates with Cl^+ ($^3P_1$ and $^3P_0$).[19] All excitation energies are given in vacuum wavenumbers. The optical resolution of the ionizing laser was 0.08 cm^{-1}, that of the dissociating laser was 0.15 cm^{-1}. Typical laser beam characteristics were 1 mJ focused by an $f = 200$ mm lens for the first laser and 150 μJ focused by an $f = 300$ mm lens for the second laser. HCl and DCl were purchased from Messer-Griesheim. The samples contained ^{35}Cl and ^{37}Cl in the natural isotope ratio; however, the data presented are for the ^{35}Cl isotope.

3. $A\ ^2\Sigma^+\ (v') \leftarrow \tilde{X}\ ^2\Pi_{3/2}\ (v'' = 0)$ Transition

In the current work, ground-state HCl^+ (DCl^+) ions are excited via the $A\ ^2\Sigma^+\ (v') \leftarrow \tilde{X}\ ^2\Pi_{3/2}\ (v'' = 0)$ transition. Note that throughout this work quantum numbers are marked by one and two primes when referring to the $A\ ^2\Sigma^+$ state and the $\tilde{X}\ ^2\Pi_{3/2}$ state of the ion and by three primes when referring to the $f\ ^3\Delta_2$ Rydberg state of neutral HCl (DCl). The ground state $^2\Pi_{3/2}$ ($v'' = 0$) of HCl^+ (DCl^+) can be described as Hund's case a.[20−23] Each rotational state of the $\tilde{X}$ state is further split by orbit−rotation coupling, also termed Λ-doubling,[24−26] into two components. These two Λ components differ in parity, *p*. According to Kopp and Hougen,[27] these rotational states can also be classified as *e*- and *f*-component, where levels with $p(-1)^{J-k} = +1$ are *e*-states, levels for which $p(-1)^{J-k} = -1$ are *f*-states ($k = 1/2$ for doublet states). The spectroscopic parameters are taken from ref 28. The actual numbers differ slightly from those previously reported in the literature.

The upper electronic state, the $A\ ^2\Sigma^+$ state, is best described in the frame of Hund's case b.[6,7,29] Each rotational state of the $A\ ^2\Sigma^+$ state is split by spin−rotation coupling into two components, with $J = 1/2$ for $N = 0$ and $J = N \pm 1/2$ for all higher *N* states. The corresponding term energies are given by[30,31]

$$F_1(N) = BN(N+1) + {}^1/_2\gamma N \quad (1)$$

and

$$F_2(N) = BN(N+1) - {}^1/_2\gamma(N+1) \quad (2)$$

where *N* is the rotational angular momentum quantum number and γ is the spin−rotation coupling constant. Note that in the $A\ ^2\Sigma^+$ state all F_1 terms correspond to *e*-states, while all F_2 terms correspond to *f*-states. The transition energies are given by

$$\tilde{\nu} = T_v + F(J') - F(J'') \quad (3)$$

where the single and double primes refer to the upper and lower electronic state, respectively; $J' = N' + 1/2$ for the F_1 component; $J' = N' - 1/2$ for the F_2 component (no F_2 level exists for $N' = 0$).

In Figure 1, we show an illustration of the allowed optical transitions of the type $A\ ^2\Sigma^+ \leftarrow \tilde{X}\ ^2\Pi_{3/2}$. Note that in both electronic states *e*- and *f*-components are alternating. The parities of neighboring states follow the order $+ + - -$. The allowed transitions are indicated by arrows. Due to the Λ-doubling in the $\tilde{X}\ ^2\Pi_{3/2}$ state, there is one set of P_1, Q_1, and R_1 branches connecting $F_1 \leftarrow F_1$ terms and one set of P_{21}, Q_{21}, and R_{21} branches connecting $F_2 \leftarrow F_1$ terms.

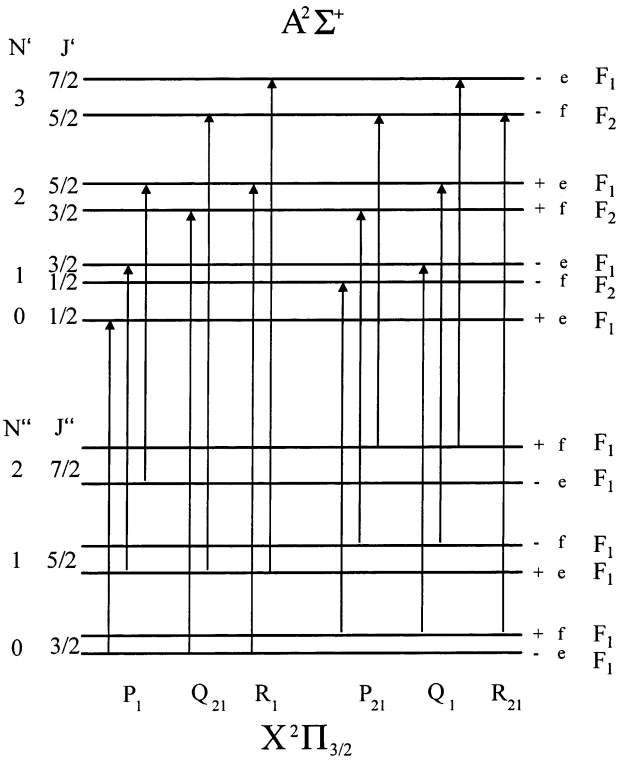

Figure 1. Illustration of the allowed optical transitions $A\ ^2\Sigma^+\ (v',J',N') \leftarrow \tilde{X}\ ^2\Pi_{3/2}\ (v'',J'',N'')$.

The intensity of any particular transition of the type $A\ ^2\Sigma^+\ (v',J',N') \leftarrow \tilde{X}\ ^2\Pi_{3/2}\ (v'',J'',N'')$ is calculated from[32,33]

$$I(v',J',N';v'',J'',N'') \sim S(J',J'')|\mu(v',J';v'',J'')|^2 \mathrm{Pop}(N'') \quad (4)$$

where $S(J',J'')$ are the Hönl−London factors for the $A\ ^2\Sigma^+(v' = 7, J', N') \leftarrow \tilde{X}\ ^2\Pi_{3/2}\ (v'' = 0, J'', N'')$ transition.[34,35] The Franck−Condon factors $|\mu(v',J';v'',J'')|^2 = |\langle\chi(v',J'|\mu|\chi(v'',J'')\rangle|^2$ are calculated explicitly by the Fourier grid Hamiltonian method[36] employing ab initio potential energy curves calculated by Dalgarno and co-workers[37] and rotational potentials as described in ref 38. The potential energy curves of the $\tilde{X}\ ^2\Pi_{3/2}$ and the $A\ ^2\Sigma^+$ state were slightly rescaled in order to match experimentally known spectroscopic[39] and thermochemical data.[40]

In the final step of the analysis, the stick spectrum containing the line positions and intensities is convoluted by a set of Lorentzian functions, with width characteristic for the lifetime of the final state. To this end, the analysis yields three pieces of information: (i) the spectroscopic parameters, (ii) the lifetime of the predissociating state, and (iii) the rotational state distribution in the $\tilde{X}$ state.

4. Results and Discussion

We have measured the predissociation spectra for various vibrational states in the $A\ ^2\Sigma^+$ state of both HCl^+ and DCl^+. The first vibrational state above the predissociation threshold is for both HCl^+ and DCl^+ relatively long-lived. Consequently, these spectra are rotationally resolved leading to highly accurate spectroscopic parameters. Also these spectra are suited best for deriving the state distribution of the initial state. For these reasons, we begin our results by discussing the PD spectra with the final states $v' = 7$ in HCl^+ and $v' = 10$ in DCl^+.

4.1. PD Spectra of HCl^+ with $v' = 7$. In previous work,[41] we have precisely located the predissociation threshold in HCl^+ as lying between the $N' = 0$ and the $N' = 1$ state of the $v' = 7$

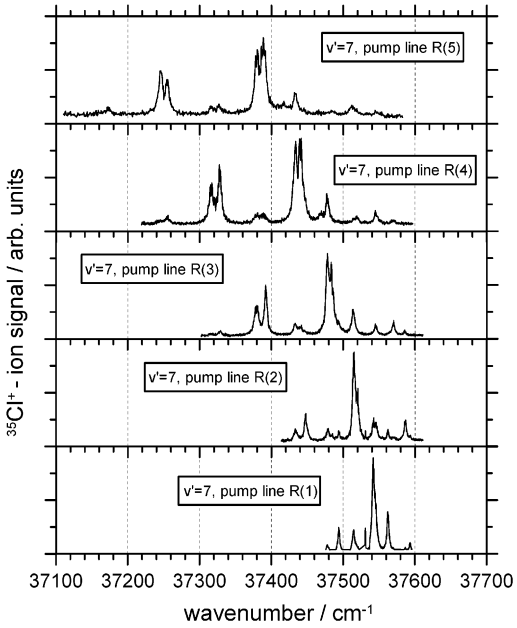

Figure 2. Predissociation spectra of the HCl^+ ion recorded via the $A\ ^2\Sigma^+$ ($v' = 7$) state.

TABLE 1: Spectroscopic Parameters of the $A\ ^2\Sigma^+$ ($v' = 7$) State of HCl^+ (in cm^{-1})

	B	γ	T_v
this work	5.230(23)	0.47(28)	37226.60(50)
ref 12	5.22		

state in HCl^+. Thus all states above the (v';N') = (7;1) state predissociate. Figure 2 shows the PD spectra $A\ ^2\Sigma^+(v' = 7) \leftarrow \tilde{X}\ ^2\Pi_{3/2}$ ($v'' = 0$) for five different pump lines in the corresponding REMPI spectrum. Some general trends are obvious. First, the line position of the dominating transitions is shifted toward lower photon energy with increasing pump line. The dominating features appear to be split into doublets. In the analysis, we have first assigned all transitions by eq 3 discussed above. Typically there are either 18 or 24 different transitions for each PD spectrum, 6 for each initial rotational state in the $\tilde{X}$ state. Consequently, we have simulated all spectra by eq 4.

4.1.1. Spectroscopic Parameters of the HCl^+ A ($v' = 7$) State. The spectroscopic parameters of the HCl^+ A ($v' = 7$) state are listed in Table 1. These parameters can be compared to other data reported in the literature. The only other source of information on the $v' = 7$ state is coming from photoelectron spectroscopy that, however, inherently has a lower resolution. Edvardsson et al. reported a value for the rotational constant $B(v' = 7) = 5.22$ cm^{-1}.[12] The He(I) PES of Yencha et al. also appears to be compatible with this number.[14] Evidently the accuracy of the current experiment surpasses that of the classical PES work.

4.1.2. Lifetime of HCl^+ in the A ($v' = 7$) State. As briefly indicated above, good agreement between observed and simulated spectrum is only achieved if the rotational dependence of the lifetime is taken into account. In going from the $R(1)$ pump line to the $R(5)$ pump line the line width of the transitions slightly increases, reflecting a decrease of the lifetime with increasing rotational quantum number N'. Figure 3 shows the lifetime of HCl^+ in the A ($v' = 7$) state as a function of N'. Shown is the range from $N' = 1$ to $N' = 7$ covered in the current PD spectra. Note that the state with $N' = 0$ does not predissociate because it lies below the PD threshold.[41] That state can, however, decay by fluorescence. In previous work we have observed the $N' = 0$ state by two photon-induced dissociation

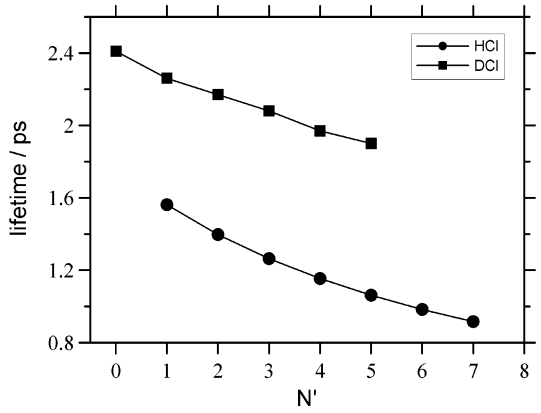

Figure 3. Predissociation lifetimes of HCl^+, $A\ ^2\Sigma^+$ ($v' = 7$), and DCl^+, $A\ ^2\Sigma^+$ ($v' = 10$).

spectroscopy. The width of that spectrum was limited by the experimental resolution.

Evidently the lifetime decreases continuously in going from $N' = 1$ to $N' = 7$. This trend is in line with theoretical calculations.[18] The absolute numbers derived from the current experiment are some what smaller than the calculated lifetimes. However, the theoretical calculations are extremely sensitive to the electronic potentials used. Very minor modification of the potential leads to significant changes in the absolute calculated lifetime. The general trends are not affected by this. The observation of a lifetime decreasing with increasing N appears to be in line with simple energetic models that rotational energy is transformed to kinetic energy of the fragments. This would probably apply in direct dissociation. In predissociation processes, the lifetime does not necessarily vary monotonically with N. Numerical wave packet calculations have shown that the lifetime $\tau(N')$ in general oscillates between limiting values.[38] There should be relatively broad regions of very low lifetime but also regions where the lifetimes run through a maximum. We have named the latter region rotational islands of stability (RIS).[38] The range of N' covered in the current work apparently is located on a decreasing part of these lifetime oscillations.

4.1.3. Rotational State Distribution of HCl^+ Ions in the $\tilde{X}\ ^2\Pi_{3/2}$ State. The HCl^+ ions investigated are formed by a REMPI process resonance enhanced via the $f\ ^3\Delta_2 \leftarrow \tilde{X}\ ^1\Sigma^+$ transition. The fact that different PD spectra are observed for different pump lines all ready implies that ions are formed in different rotational states depending on the REMPI pump line. From a detailed analysis of eq 4 the rotational state distribution Pop(N'') has been derived and plotted in Figure 4. In general the population is concentrated in two rotational states. With increasing pump line the distribution is shifted toward higher rotational quantum numbers.

The trends operative in the distribution are discussed in comparison with the change in angular momentum in the final step of the REMPI process. For the $R(1)$ pump line most of the population is observed in the $N'' = 0$ state of the ion. This corresponds to $J'' = 3/2$. Since for the $R(1)$ pump line $J''' = 2$ and $N''' = 0$ in the intermediate Rydberg state ($f\ ^3\Delta_2$), we conclude that $\Delta J = J'' - J''' = -1/2$ dominates in the ejection of the photoelectron. For the $R(2)$ pump line $N'' = 1$ dominates in the state distribution of the $\tilde{X}$ state, which again corresponds to a $\Delta J = -1/2$ transition. For the $R(3)$ pump line $N'' = 2$ and $N'' = 3$ have comparable intensity, thus $\Delta J = -1/2$ and $\Delta J = +1/2$ carry similar intensity. For $R(4)$ and $R(5)$ pump lines, $N'' = 4$ and $N'' = 5$ dominate, indicating a preference for $\Delta J = +1/2$ transitions. Thus, the general trend goes from $\Delta J = -1/2$ to $\Delta J = +1/2$ transitions with increasing pump line. As pointed

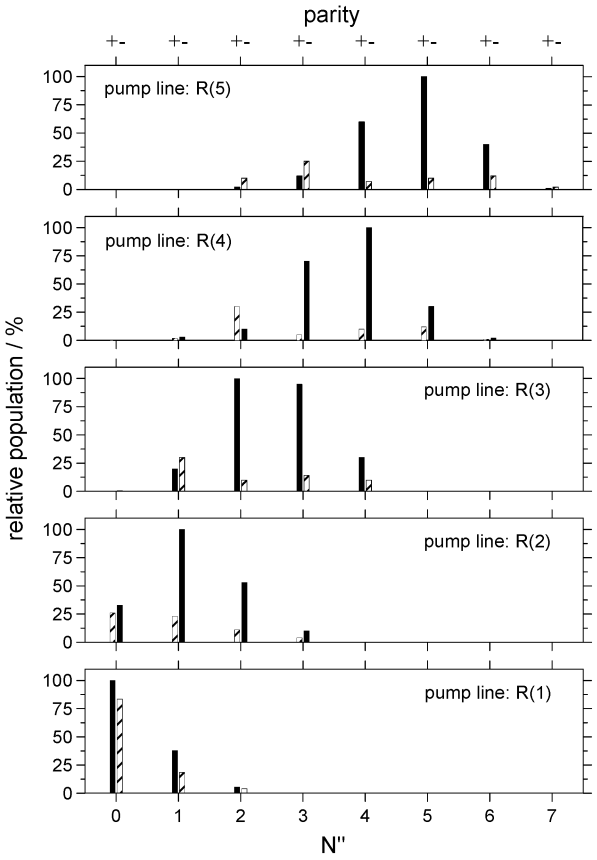

Figure 4. Rotational state distribution of HCl^+ ions in the $\tilde{X}\ ^2\Pi_{3/2}$ state for five different pump lines in the REMPI spectrum.

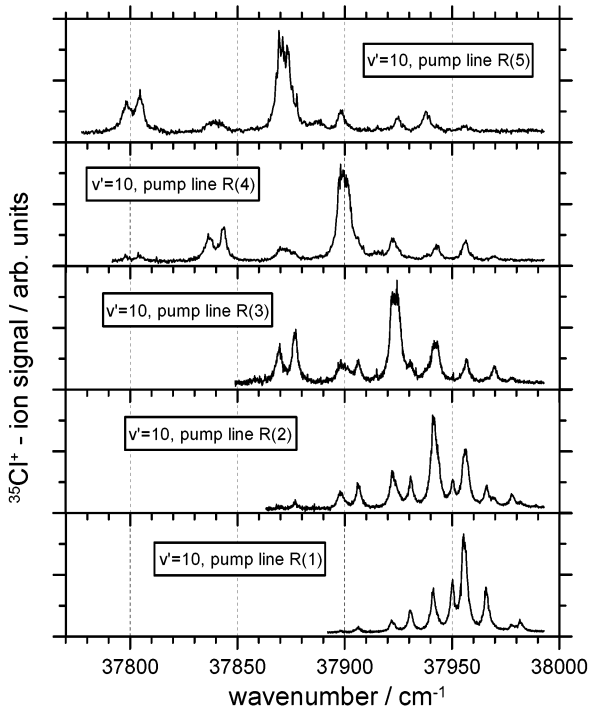

Figure 5. Predissociation spectra of the DCl^+ ion recorded via the $A\ ^2\Sigma^+$ ($v' = 10$) state.

TABLE 2: Spectroscopic Parameters of the $A\ ^2\Sigma^+$ ($v' = 10$) State of DCl^+ (in cm^{-1})

B	γ	T_v
2.676(14)	0.235(65)	37636.00(50)

out above, the current PD spectra clearly allow to distinguish the parity states associated with a Λ-doublet in the $\tilde{X}$ state. This is possible despite the fact that the Λ-doubling itself amounts to only a fraction of 1 cm^{-1} for the lowest J state. The key point is the projection of the $\tilde{X}$ state onto the A state with a significant change in spectroscopic parameters.

At this point we briefly recall the basis for parity preferences in the 2+1 REMPI process.[42,43] In a simple picture the $f\ ^3\Delta_2$ Rydberg state in HCl (DCl) arises from a ($4p\pi$) electron configuration. For a Rydberg electron of p-character, the photoelectron would be expected to be ejected as an s- or a d-wave with a change in parity of the molecular core. In this case for a $R(1)$ pump line in the REMPI spectrum ions would be expected to be formed with parity +. Wang and McKoy[44] showed that the $F\ ^1\Delta_2$ state of HCl has in fact has 95.25% p and 4.7% d character. In analogy to HBr[6] a very similar angular momentum composition can be expected for the $f\ ^3\Delta_2$ state of HCl, where the d-character of the Rydberg electron would give rise to photoelectrons with partial wave character p and f. For the $R(1)$ pump line in the REMPI spectrum this would lead to ions with parity −. Since the d-character of the Rydberg electron is small, one would expect that the favored parity state clearly dominates. For the $R(1)$ pump line, this dominance is not observed. In fact, the two parity states are populated with very similar intensity. Note, that the expected parity alternates between + and − for consecutive pump lines. For the higher pump lines $R(2)$ to $R(5)$, it is appropriate to conclude a dominance of one particular parity state. The ratio of expected to unexpected parity will be further discussed in a later section.

4.2. PD Spectra of DCl^+ with $v' = 10$. While in the HCl^+ A state, the predissociation threshold has been located precisely as lying between the $N' = 0$ and $N' = 1$ state of $v' = 7$.[41] This threshold has not been observed directly in DCl^+. Since in the Born−Oppenheimer approximation the electronic potential energy curves are identical, the predissociation threshold can be calculated to occur between the $v' = 9$ and $v' = 10$ state of DCl^+ (A state). Thus $v' = 10$ is the first state for which all rotational states predissociate.

Figure 5 shows the predissociation spectra of DCl^+ with $v' = 10$ recorded via the pump lines $R(1)$ to $R(5)$ of the corresponding REMPI spectrum. As expected the overall trends of these spectra are very similar to HCl^+ (Figure 2). However, the signal-to-noise ratio is not as good. The reason for this is connected to the Franck−Condon factor, which is significantly smaller in DCl^+, $v' = 10$. This leads to the fact that the absolute fragment yield is typically only about 2% in DCl^+, $v' = 10$. For HCl^+, $v' = 7$ fragment yields up to 20% were observed. In the analysis of the DCl^+ PD spectra we proceed analogous to the HCl^+.

4.2.1. Spectroscopic Parameters of the DCl^+ A ($v' = 10$) State. The spectroscopic parameters of DCl^+, $v' = 10$ are listed in Table 2. To the best of our knowledge there is no other direct measurement of these parameters in the literature. By extrapolation from data for lower v states, Edvardsson et al. predicted a value of 2.62 cm^{-1} for $B(v' = 10)$,[12] which is outside our uncertainty (2.676(14) cm^{-1}). Also note, that the $v' = 10$ state cannot be observed by laser-induced fluorescence nor by emission spectroscopy.

4.2.2. Lifetime of DCl^+ in $v' = 10$. The line width of the DCl^+ PD spectra for $v' = 10$ is about a factor of 2 smaller than in HCl^+, $v' = 7$, indicating a larger predissociation lifetime. For the range of rotational states from $N' = 0$ to $N' = 5$, the predissociation lifetime is found to decrease smoothly from $\tau(N' = 0) = 2.41$ ps to $\tau(N' = 5) = 1.9$ ps. These data are also

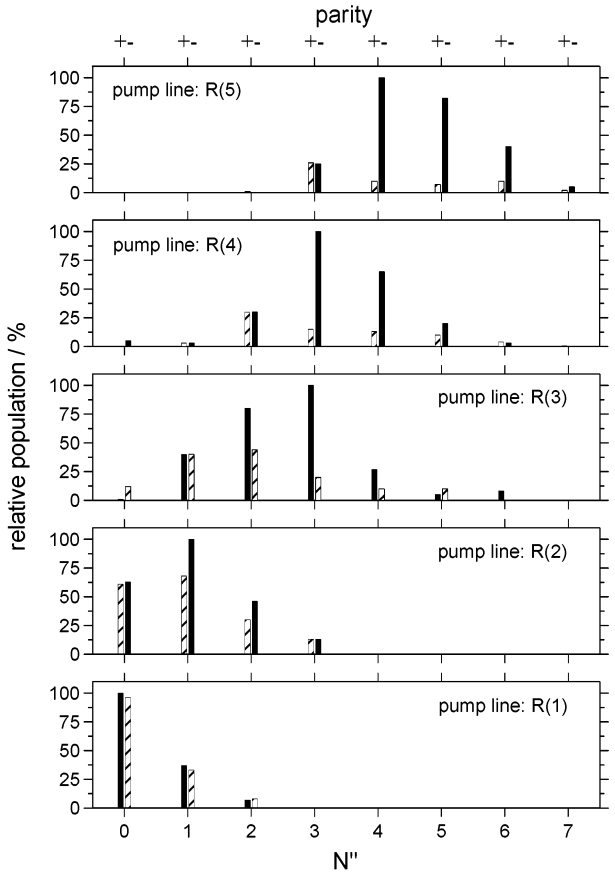

Figure 6. Rotational state distribution of DCl^+ ions in the $\tilde{X}\ ^2\Pi_{3/2}$ state for five different pump lines in the REMPI spectrum.

included in Figure 3 discussed above. The observation of the lifetimes being systematically larger than in HCl^+ is surprising at first glance. In the case of the HCl^+ the rotational states discussed are directly at the threshold of predissociation (the $N = 1$ state is the first state that predissociates). In the DCl^+ on the other hand, the first quantum state discussed ($N = 0$) is already about 150 cm^{-1} above the predissociation threshold. Thus one might expect that the predissociation lifetime in DCl^+ is shorter than in HCl^+. On the other hand, quite often predissociation times are longer in the heavier isotopomer.[32,45] This does not necessarily have to be the case, since predissociation dynamics in general is governed by characteristics of the wave functions involved. In fact, the observation of lifetimes being larger in the threshold region for DCl^+ as compared to HCl^+ is also predicted by wave packet calculations.[46]

4.2.3. Rotational State Distribution of DCl^+ in the $\tilde{X}\ ^2\Pi_{3/2}$ State. From the analysis of the spectra presented in Figure 5, the population of the DCl^+ ions in the $\tilde{X}\ ^2\Pi_{3/2}$state was derived. These rotational state distributions are plotted in Figure 6. The overall trends observed are very similar to HCl^+. In general two rotational states carry more than two-thirds of the total population. The center of the rotational state distribution is shifted toward higher N' with increasing pump line. Specific differences between the state distribution in DCl^+ and HCl^+ are however revealed when looking at the ratio of expected to unexpected parity states. For illustration, we show in Figure 7 the fraction of unexpected parity states in percent as a function of the rotational quantum number in the resonant Rydberg state of the REMPI process, N'''. This quantum number is synonymous with a specific pump line (e.g., the $R(1)$ pump line leads to $N''' = 0$). For both HCl^+ and DCl^+ the fraction of unexpected parity in general decreases with increasing N''', but for HCl^+

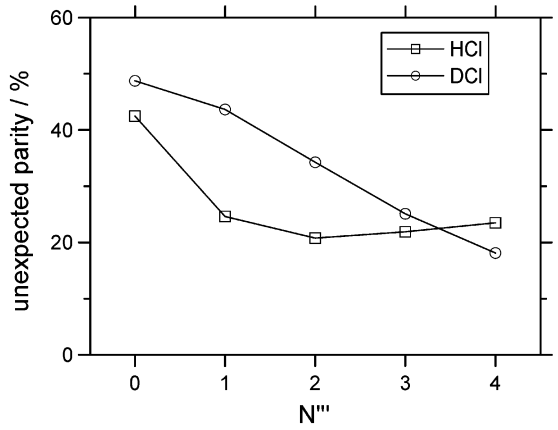

Figure 7. Fraction of unexpected parity states in HCl^+ and DCl^+.

the decrease is steeper. To the best of our knowledge no other information is available in the literature for this specific REMPI process. Wang et al. have calculated parity resolved rotational state distributions for HCl^+ ions formed via the $F\ ^1\Delta_2 \leftarrow \tilde{X}\ ^1\Sigma^+$ transition in a $(2+1')$ two color REMPI process.[44] For the $S(0)$ pump line, it was found that rotational states in the ion $\tilde{X}$ state are populated with the intensity decreasing from $N'' = 0$ to $N'' = 4$. This general trend is in principle compatible with the current results for the $R(1)$ pump line. However, for the current $R(1)$ pump line data (via $f\ ^3\Delta_2$), the fraction of unexpected parity states is significantly higher than for the calculated $S(0)$ data (via $F\ ^1\Delta_2$). For a given REMPI transition $R(1)$ and $S(0)$ pump lines lead to almost identical state distributions; however, the dominating parity is reversed. For intermediate Rydberg states $f\ ^3\Delta_2$ and $F\ ^1\Delta_2$, a major difference arises from the fact that $N'' = 0$ correlates with $J'' = 3/2$ in a $^2\Pi_{3/2}$ state, but $N'' = 0$ correlates with $J'' = 1/2$ in a $^2\Pi_{1/2}$ state. Thus for both a $R(1)$ and a $S(0)$ pump line, a $\Delta J = J'' - J''' = -3/2$ transition is possible via the $F\ ^1\Delta_2$ state; it is not possible via the $f\ ^3\Delta_2$. In the latter case, which applies in the current work, this "missing" intensity in part appears as unexpected parity in the $N'' = 0$ state. We have made the same observation in HBr^+ for which we investigated both the $f\ ^3\Delta_2 \leftarrow \tilde{X}\ ^1\Sigma^+$ and the $F\ ^1\Delta_2 \leftarrow \tilde{X}\ ^1\Sigma^+$ REMPI processes.[8]

Wang and McKoy[44] showed that the population of unexpected parity states arises from the nonspherical molecular ion potential. Here, the decrease in the fraction of unexpected parity with increasing rotational quantum number in the Rydberg state might be rationalized as being due to a decrease in the anisotropy. It is interesting to note that in a plot of the fraction of unexpected parity versus the rotational energy the data for HCl^+ and DCl^+ are much closer than in the plot versus the rotational quantum number. An alternative point of view would be that the angular momentum composition of the Rydberg state could effectively depend on the rotational angular momentum. In general, different pump lines in the REMPI spectrum will be associated with photoelectrons of different kinetic energy. It also appears possible that the transition matrix elements connecting to the different parities have different energy dependence. Hints at such an effect have been implied by Wang and McKoy,[43,44] however, for significantly larger energy differences. Clearly further theoretical work is required to resolve these questions.

For HCl^+ the fraction of unexpected parity appears to increase again for $N''' = 3$ and 4. However, within the experimental uncertainty of $\pm 5\%$, the data could also imply that for high N''' a limiting fraction of about 20% is reached. Further experiments for higher rotational states would be required to resolve this question. In general for each pump line changes in

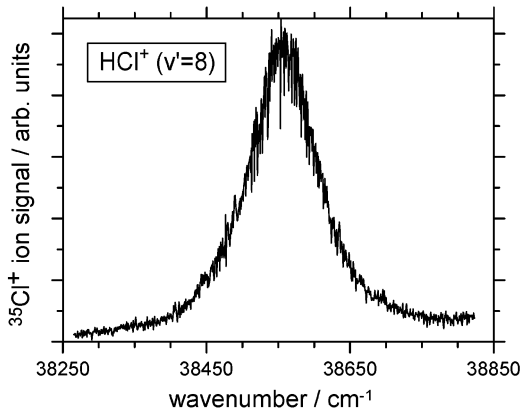

Figure 8. Predissociation spectrum of the HCl^+ ion recorded via the $A\ ^2\Sigma^+$ ($v' = 8$) state.

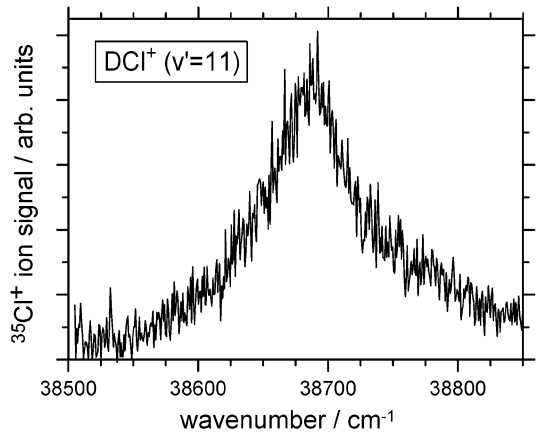

Figure 9. Predissociation spectrum of the DCl^+ ion recorded via the $A\ ^2\Sigma^+$ ($v' = 11$) state.

the angular momentum of $\Delta J = J'' - J''' = -3/2$, $-1/2$, $1/2$, and $3/2$ are observed. There are pronounced differences in the weight of these contributions. For the lowest pump line the relative fraction of unexpected parity state is largest for the $\Delta J = -1/2$ transition. The decrease in the over all fraction of unexpected parity with increasing pump line is basically due to a decrease in $\Delta J = -1/2$, $1/2$, and $3/2$. Only the $\Delta J = -3/2$ transition does not decrease with increasing pump line. In fact for the HCl^+ the $\Delta J = -3/2$ transition markedly increases from pump line $R(2)$ to $R(4)$.

4.3. PD Spectra of HCl^+ and DCl^+ via Higher Vibrational States. The PD spectra for HCl^+, $v' = 7$, and DCl^+, $v' = 10$ are clearly rotationally resolved because of the corresponding final state lifetime. In the following, we discuss the PD spectra of HCl^+, $v' = 8$, 9, and 10 and DCl^+, $v' = 11$ and 12. Typical spectra are shown in Figures 8 (HCl^+, $v' = 8$) and 9 (DCl^+, $v' = 11$). Evidently the spectra are not rotationally resolved indicating a dramatically reduced lifetime. Again all spectra have been simulated by the procedure described above. For the $\tilde{X}$ state, the same spectroscopic parameters and populations are used. At this point we are mainly interested in the lifetime for predissociation in the A (v') states. In the analysis, each particular PD spectrum was simulated with a single lifetime for all final states contributing to the spectrum. The lifetime derived are listed in Table 3 for HCl^+ and in Table 4 for DCl^+, both in comparison with information from the literature. For HCl^+ the lifetime decreases by a factor of 20 from $v' = 7$ to $v' = 8$. But for $v' = 9$ and $v' = 10$ the lifetime increases again. For DCl^+ the lifetime also decreases by about a factor of 20 from $v' = 10$ to $v' = 11$, but it further decreases slightly to $v' = 12$. We have not been able to record PD spectra of DCl^+ with $v' = 13$ or larger due to low signal levels. The decrease and increase of the lifetime is believed to be due to a general phenomenon connected to the interaction of the quasi-bound wave function in the A state and the outgoing wave function of the repulsive states. Only if the overlap of these wave functions is favorable, predissociation occurs fast, else it may occur only slow.

TABLE 3: Predissociation Lifetimes of HCl^+ as a Function of the Vibrational Quantum Number v' in the A State (in ps)[a]

state	this work	ref 12	ref 13	ref 18
$v' = 7$	1.56(5)[b]	>0.1	0.039	4.3
$v' = 8$	0.063(12)	0.057	0.031	0.095
$v' = 9$	0.139(21)	0.1	0.055	0.825
$v' = 10$	0.171(23)	0.13	0.219	0.351

[a] For comparison, data from the literature are included. [b] Data for the $N' = 1$ state.

TABLE 4: Predissociation Lifetimes of DCl^+ as a Function of the Vibrational Quantum Number v' in the A State (in ps)

state	this work
$v' = 10$	2.41(6)[a]
$v' = 11$	0.089(18)
$v' = 12$	0.076(17)

[a] Data for the $N' = 0$ state.

As indicated above, the analysis of these PD spectra is again based on spectroscopic parameters of both states involved. The question arises whether a rotational constant B has any physical meaning for a state with lifetime on the order of 100 fs. In fact for HCl^+ we have also recorded PD spectra for higher pump lines, which clearly exhibit pronounced shoulders. The analysis leads to rotational constants in HCl^+ of $B(v' = 8) = 4.9 \pm 2.0$ cm^{-1}, $B(v' = 9) = 4.5 \pm 0.5$ cm^{-1}, and $B(v' = 10) = 4.5 \pm 1.0$ cm^{-1}. For the DCl^+ we have employed $B(v' = 11) = 2.6 \pm 1.0$ cm^{-1}, and $B(v' = 12) = 2.4 \pm 1.0$ cm^{-1}. However, for the DCl^+ our data are not very sensitive to these numbers. We also note that the PD spectra recorded via higher pump lines suggest a slight decrease in lifetime with increasing N' for $v' = 8$, 9, and 10 in HCl^+. However, the effect is small and tentative. For the DCl^+ we do not have any information of this kind.

5. Summary

The state-selective predissociation spectroscopy of HCl^+ and DCl^+ ions has been investigated in a two-color double-resonance experiment. In the first step of the experiment ions are formed in the vibronic ground state via the $f\ ^3\Delta_2 \leftarrow \tilde{X}\ ^1\Sigma^+$ REMPI process. In the second step the predissociation of these ions is investigated via the $A\ ^2\Sigma^+$ (v') $\leftarrow \tilde{X}\ ^2\Pi_{3/2}$ ($v'' = 0$) transition. There are two ways to look at this experiment. From one point the REMPI process provides access to HCl^+ and DCl^+ ions with rotational state distributions, which can be characterized or even utilized in consecutive experiments. From the other point, the state-selective predissociation provides detailed information on the REMPI process itself.

The current work clearly shows that ions can be formed in rather narrow rotational state distributions. The center of these distributions can be shifted from $N' = 0$ to about $N' = 5$ by choosing the appropriate pump line in the REMPI process. There is no fundamental limit for going to even higher pump lines, but there will be intensity restrictions for experiments performed at a specific temperature. The state distributions observed in the current work are very important for the study of state-selected ion−molecule reactions.[33,47−52] The rotational state

distributions obtained exhibit a very large fraction of unexpected parity states for the lowest pump line. This fraction decreases with increasing pump line. Tentatively this is assigned to a concomitant decrease in the anisotropy of the effective potential with increasing rotational quantum number. We hope that the current results stimulate further theoretical work along the photoionization dynamics of HCl and DCl.

Acknowledgment. Support of this work by the Deutsche Forschungsgemeinschaft (We 1330/3) is gratefully acknowledged. We would also like to thank Prof. H. Baumgärtel and Prof. E. Illenberger for the loan of technical equipment. K.M.W. wishes to thank Prof. Tomas Baer cordially for introducing him to the field of ion chemistry and for many scientific and personal discussions over the past 15 years.

References and Notes

(1) Baer, T.; Hase, W. L. *Unimolecular Reaction Dynamics*; Oxford University Press: New York, 1996.
(2) Armentrout, P. B.; Baer, T. *J. Phys. Chem.* **1996**, *100*, 12866.
(3) Troe, J., Baer, M., Ng, C.-Y., Eds. *State-Selected and State-to-State Ion−Molecule Reaction Dynamics, Part 2*: *Theory*, 82nd ed.; John Wiley & Sons: New York, 1992; p 485.
(4) Anderson, S. L. *Adv. Chem. Phys.* **1992**, *82*, 177.
(5) Xie, J.; Zare, R. N. *Chem. Phys. Lett*. **1989**, *159*, 399.
(6) Wales, N. P. L.; Buma, W. J.; de Laange, C. A.; Lefebvre-Brion, H.; Wang, K.; McKoy, V. *J. Chem. Phys.* **1996**, *104*, 4911.
(7) de Beer, E.; Buma, W. J.; de Lange, C. A. *J. Chem. Phys.* **1993**, *99*, 3252.
(8) Penno, M.; Weitzel, K. M. *Z. Phys. Chem.* **2004**, *218*, 311.
(9) Green, D. S.; Bickel, G. A.; Wallace, S. C. *J. Mol. Spectrosc.* **1991**, *150*, 303.
(10) Green, D. S.; Bickel, G. A.; Wallace, S. C. *J. Mol. Spectrosc.* **1991**, *150*, 354.
(11) Green, D. S.; Bickel, G. A.; Wallace, S. C. *J. Mol. Spectrosc.* **1991**, *150*, 388.
(12) Edvardsson, D.; Baltzer, P.; Karlsson, L.; Lundqvist, M.; Wannberg, B. *J. Electron Spectrosc*. **1995**, *73*, 105.
(13) Yencha, A. J.; McConkey, A. G.; Dawber, G.; Avaldi, L.; MacDonald, M. A.; King, G. C.; Hall, R. I. *J. Electron Spectrosc*. **1995**, *73*, 217.
(14) Yencha, A. J.; Cormack, A. J.; Donovan, R. J.; Hopkirk, A.; King, G. C. *Chem. Phys*. **1998**, *238*, 109.
(15) de Beer, E.; Koenders, B. G.; Koopmans, M. P.; De Lange, C. A. *J. Chem. Soc., Faraday Trans.* **1990**, *86*, 2035.
(16) Penno, M.; Holzwarth, A.; Weitzel, K. M. *Mol. Phys.* **1999**, *97*, 43.
(17) Penno, M.; Holzwarth, A.; Weitzel, K. M. *J. Phys. Chem. A* **1998**, *102*, 1927.
(18) Korolkov, M. V.; Weitzel, K. M.; Peyerimhoff, S. D. *Int. J. Mass Spectrom.* **2000**, *201*, 109.
(19) Banichevich, A.; Klotz, R.; Peyerimhoff, S. D. *Mol. Phys*. **1992**, *75*, 173.
(20) Ibuki, T.; Sato, N.; Iwata, S. *J. Chem. Phys.* **1983**, *79*, 4805.
(21) Pratt, S. T. *J. Chem. Phys.* **1994**, *101*, 8302.
(22) Norling, F. *Z. Phys.* **1935**, *95*, 179.
(23) Mulliken, R. S. *Phys. Rev.* **1928**, *32*, 388.
(24) Hill, E.; Van Vleck, J. H. *Phys. Rev.* **1928**, *32*, 250.
(25) Mulliken, R. S.; Christy, A. *Phys. Rev.* **1931**, *38*, 87.
(26) Vleck, J. H. V. *Phys. Rev.* **1929**, *33*, 467.
(27) Kopp, I.; Hougen, J. T. *Can. J. Phys.* **1967**, *45*, 2581.
(28) Michel, M. Dissertation, Freie Universität Berlin, 2003.
(29) Lefebvre-Brion, H.; Keller, F. *J. Chem. Phys.* **1989**, *90*, 7176.
(30) Johns, J. W. C. *J. Mol. Spectros.* **1970**, *36*, 488.
(31) Kovacs, I. *Rotational Structure in the Spectra of Diatomic Molecules*; American Elsevier: New York, 1969.
(32) Lefebvre-Brion, H.; Field, R. W. *Perturbations in the Spectra of Diatomic Molecules*; Academic Press: Orlando, FL, 1986.
(33) Michel, M.; Korolkov, M. V.; Malow, M.; Brembs, K.; Weitzel, K. M. *Phys. Chem. Chem. Phys.* **2001**, *3*, 2253.
(34) Earls, L. T. *Phys. Rev.* **1935**, *48*, 423.
(35) Zare, R. N. *Angular Momentum*; John Wiley & Sons: New York, 1988.
(36) Marston, C. C.; Balint-Kurti, G. G. *J. Chem. Phys.* **1989**, *91*, 3571.
(37) Pradhan, A. D.; Kirby, K. P.; Dalgarno, A. *J. Chem. Phys*. **1991**, *95*, 9009.
(38) Korolkov, M. V.; Weitzel, K. M. *Chem. Phys. Lett*. **2001**, *336*, 303.
(39) Saenger, K. L.; Zare, R. N.; Mathews, C. W. *J. Mol. Spectrosc*. **1976**, *61*, 216.
(40) Lias, S. G.; Bartmess, J. E.; Liebman, J. F.; Homes, J. L.; Levine, R. D.; Mallard, W. G. **1988**, *17* (Suppl. 1).
(41) Michel, M.; Korolkov, M. V.; Weitzel, K. M. *Phys. Chem. Chem. Phys.* **2002**, *4*, 4083.
(42) Xie, J.; Zare, R. N. *J. Chem. Phys*. **1990**, *93*, 3033.
(43) Wang, K.; McKoy, V. *J. Chem. Phys.* **1991**, *95*, 4977.
(44) Wang, K.; McKoy, V. *J. Chem. Phys.* **1991**, *95*, 8718.
(45) Wheeler, M. D.; OrrEwing, A. J.; Ashfold, M. N. R. *J. Chem. Phys.* **1997**, *107*, 7591.
(46) Weitzel, K. M.; Korolkov, M. V. Manuscript in preparation.
(47) Malow, M.; Brembs, K.; Weitzel, K. M. *Z. Phys. Chem.* **2001**, *215*, 737.
(48) Anderson, S. L. *Acc. Chem. Res.* **1997**, *30*, 28.
(49) Smith, M. A. *Int. Rev. Phys. Chem.* **1998**, *17*, 35.
(50) Belikov, A. E.; Mullen, C.; Smith, M. A. *J. Chem. Phys.* **2001**, *114*, 6625.
(51) Belikov, A. E.; Smith, M. A. *Chem. Phys. Lett*. **2002**, *358*, 57.
(52) Belikov, A. E.; Smith, M. A. *Chem. Phys. Lett*. **2004**, *387*, 7.